



Seismic Performance Evaluation of Cold-Formed Steel Framed Shear Walls using In-Frame Corrugated Steel Sheets

Xing Lan¹, Wenying Zhang², Mahsa Mahdavian³, Cheng Yu⁴

Abstract

This paper presents experiments and finite element analysis of an innovative cold-formed steel framed shear wall with corrugated steel sheathing. The novel shear wall is high strength, non-combustible, and is equal in width with adjacent walls. Full-scale monotonic and cyclic tests were conducted on bearing walls and shear walls under combined lateral and gravity loading. The strength of the novel shear wall is higher than currently code certified shear walls in AISI S400-15 so that it could be employed for mid-rise buildings in areas that are prone to high seismic and wind loads. It was also found that the shear strength of bearing wall was approximately one third of the shear strength of shear wall, which proves that bearing walls provide significant shear resistance in a structure. In finite element analysis, shear wall models were first simulated and verified in OpenSees software, then nonlinear static and dynamic analysis were performed in OpenSees software according to the methodology recommended by FEMA P695. The objective of numerical analysis was to evaluate and quantify seismic performance factors of this new lateral force resisting system. The seismic performance evaluation results verified that the existing seismic performance factors for conventional light framed shear wall systems were appropriate for the novel cold-formed steel shear wall systems.

1. Introduction

Mid-rise cold-formed steel (CFS) structures are one of the economic solutions for increasing housing demand, especially in highly populated areas. Due to the non-combustibility material requirement by IBC for Types I and II construction, shear walls with flat steel sheets and cross bracing shear walls are the only available options for mid-rise buildings. However, the low strength of the shear wall with flat steel sheets significantly obstructs the application of cold-formed steels in mid-rise buildings, particularly in areas subjected to high seismic and/or strong wind hazards. Non-combustible CFS shear walls with high structural performance are in great need in the mid-rise construction market.

¹ Structural Engineer, Mako Steel Inc., <xing@makosteel.com>

² Graduate Research Assistant, Tongji University, <wenyingchangan@163.com >

³ Research Engineer, Verco Decking Inc., < mahsa_mahdavian@yahoo.com >

⁴ Professor, University of North Texas, < cheng.yu@unt.edu >

Replacing flat sheet panels with corrugated steel sheets is a solution to improve shear walls strength. Shear walls with corrugated steel sheets have been a subject of interest for multiple researchers in recent years. These researchers have investigated a wide range of parameters and their effects on the performance of the shear walls such as: sheathing and framing member thickness (Stojadinovic and Tipping 2007, Yu et al. 2009), fastener size and spacing (Stojadinovic and Tipping 2007), wall aspect ratio (Mahsa Mahdavian 2016), opening patterns on corrugated steel sheathing (Yu 2013, Mahsa Mahdavian 2016), gravity load effects on shear walls (Mahsa Mahdavian 2016, Wenying Zhang 2016), and etc. All of the experimental results indicated that shear walls with corrugated steel sheets can yield higher shear strength and stiffness than current code certified shear walls.

Among all of these researchers, Zhang (2016) conducted 4 shear wall and 4 bearing wall tests under combined lateral and gravity loading. It was concluded that the gravity load would increase the shear strength and initial stiffness of the wall. In addition, a 7% collapse drift limit for the new shear wall system with corrugated steel sheathing was also suggested by Zhang (2016). In finite element modeling, Zhang (2017) adopted FEMA P695 methodology for the performance evaluation of office and hotel building archetypes to verify the seismic performance factors of the newly proposed shear walls systems. Seismic performance factors ($R=C_d=6.5$ and $\Omega = 3.0$) obtained from the structure seismic performance evaluation were concluded to be appropriate for these newly proposed shear wall systems.

The shear walls studied by Zhang and other researchers has the corrugated steel sheathing attached to the outside (sheet-out shear wall) of the framing members causing unequal wall thickness with the adjacent walls. This would result in difficulties of design and installation of finish materials. Therefore in 2016, Mahdavian introduced a new shear wall system with corrugated steel sheathing attached to the framing from inside (sheet-in shear wall) which resolved the previously discussed problems.

This paper follows up on Mahdavian (2016) and Zhang(2016, 2017) research by conducting monotonic and cyclic tests of sheet-in shear walls under combined lateral and gravity loads to investigate the effects of gravity loads on sheet-in shear walls and bearing walls. Seismic performance evaluation was performed on 3 office archetypes by following FEMA P695 methodology on these novel sheet-in shear wall lateral force resisting system, and the results are reported herein.

2. Test Program

2.1 Test Setup

Shear wall tests were conducted in the Structural Laboratory at the University of North Texas. The structural steel testing frame was equipped with a MTS 35 kip hydraulic actuator with a 10 in. stroke. A total of 5,384 pounds of gravity load was calculated based on the two-story CFS-NEES office building((Madsen, Nakata, Schafer, 2011). This weight was divided into two equal parts and added on each side of the wall by using weight boxes equipped with sand bags and held by steel chains at the loading beam. Weight boxes were held approximately 5 inches off the ground before the test. Contacts between weight boxes and shear walls were eliminated by using a supporting frame. The applied force and displacements were recorded instantaneously during each test. Details of the 8' x 4' wall test setup are shown in Fig. 1.

The lateral loading was applied directly to the T-shaped loading beam by the actuator. The loading beam was attached to the web of the top track using screw connections. The web of the T-shape beam was placed in the gap between the rollers located at the top of the testing frame to prevent out-of-plane movement of the wall. The rotation of the rollers was able to reduce the friction generated by the movement of the T-shape beam during the loading process and were also able to guide the loading T-shape beam.

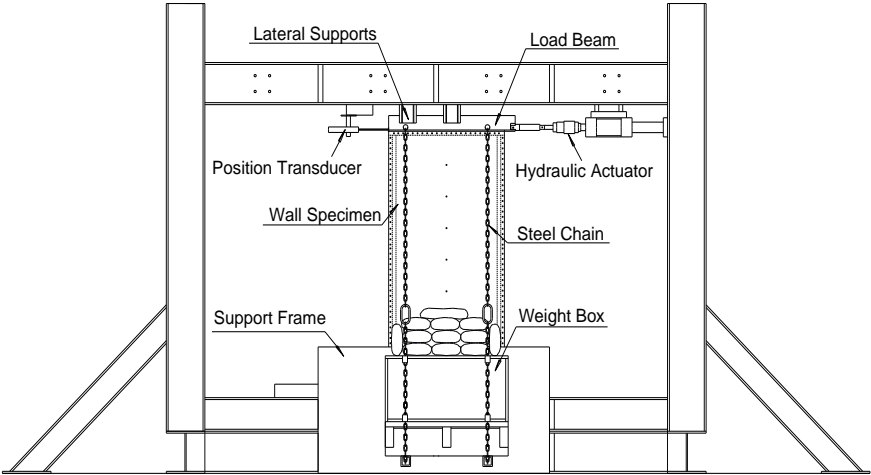


Fig. 1: Test Setup

2.2 Test Method

Both monotonic and cyclic tests were conducted on bearing walls and shear walls. The procedure of the monotonic tests was in accordance with ASTM E564 (2012) “Standard Practice for Static Load Test for Shear Resistance of Framed Walls for Buildings”. The procedure of cyclic tests referred to CUREE protocol with 0.2 Hz (5 seconds) loading frequency which was in accordance with Method C in ASTM E2126 (2012) “Standard Test Methods for Cyclic (Reversed) Load Test for Shear Resistance of Vertical Elements of the Lateral Force Resisting Systems for Buildings.” The standard CUREE loading includes 40 cycles with specific displacement amplitudes, as shown in Fig. 2. The gravity load was applied to the wall specimens prior to the lateral loading. The lateral loading was applied to the wall using displacement controlled loading method.

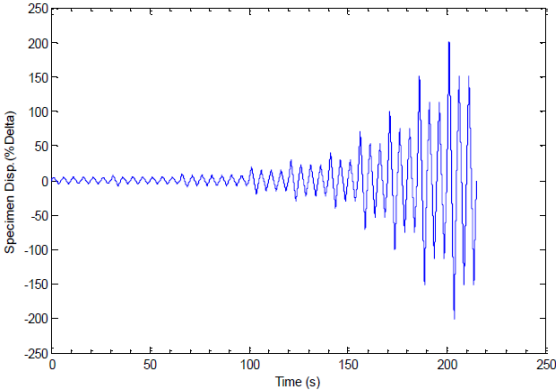


Fig. 2: CUREE Loading History Diagram (0.2 Hz)

2.3 Test Specimens

Test specimens are labeled by following rules: “Wall Width (ft.) x Wall Height (ft.) x Framing Member Thickness (mil) x Sheathing Thickness (mil) – Test Number.” Text Matrix is summarized in Table 1.

It needs to be aware of that tracks were used to replace stud framing members in sheet-in walls so that the corrugated steel sheets were able to be installed inside the frame. Simpson Strong-tie S/HD 15S Hold-downs in shear walls were screwed outside of the vertical chord tracks by No. 14x1 in. hex washer head self-drilling screws. 362T150-68 were used as top and bottom tracks, the 300T200-68 field vertical track was specially manufactured for the purpose of these walls. 3 of 27 mil Verco Decking SV36 corrugated steel sheets were used and attached by #12 screws at seams and at panel to frame connection. The corrugated steel sheet profile is shown in Fig. 3.

Table 1: Test Matrix

Test Label	Wall Type	Test protocol (M/C)	Gravity Load	Hold-down	Vertical chord tracks
4x8x68x27 - T#1	Bearing wall	M	Y	N	1
4x8x68x27 - T#1	Bearing wall	C	Y	N	1
4x8x68x27 - T#2	Bearing wall	C	Y	N	1
4x8x68x27 - T#1	Shear wall	M	Y	Y	2
4x8x68x27 - T#1	Shear wall	C	Y	Y	2
4x8x68x27 - T#2	Shear wall	C	Y	Y	2

Note: M - Monotonic loading, C - Cyclic loading.

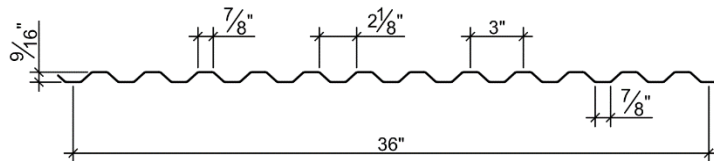


Fig. 3: Verco Decking SV36 Sheathing Profile

2.4 Material Properties

Coupon tests of each member were conducted according to the ASTM A370 (2006) “Standard Test Methods and Definitions for Mechanical Testing of Steel Products” to obtain the actual properties of all test materials. A total of three coupon tests were performed for each member, and the average results are provided in Table 2.

Table 2: Material properties of Wall Components

Member	Yield Stress F_y (ksi)	Tensile Strength F_u (Ksi)
362T150-68	53.15	70.07
350T125-68	57.49	74.42
300T200-68	55.00	71.07
27mil Verco Decking SV36	86.09	89.93

2.5 Test Results & Discussions

2.5.1 Wall Behaviors under Monotonic Loading

For the bearing wall under monotonic loading, it was observed that the vertical chord tracks and the bottom track on the tension side was lift up due to no hold-downs being in place, while the vertical chord tracks and the bottom track on the compression side buckled. No screw failures were observed. The maximum displacement was set to 7.2 in. and was equivalent to 7.5% story drift. The bearing wall specimen was able to carry the gravity load without collapse during the entire loading process. The failures of the bearing wall specimen under monotonic loading are shown in Fig. 4.

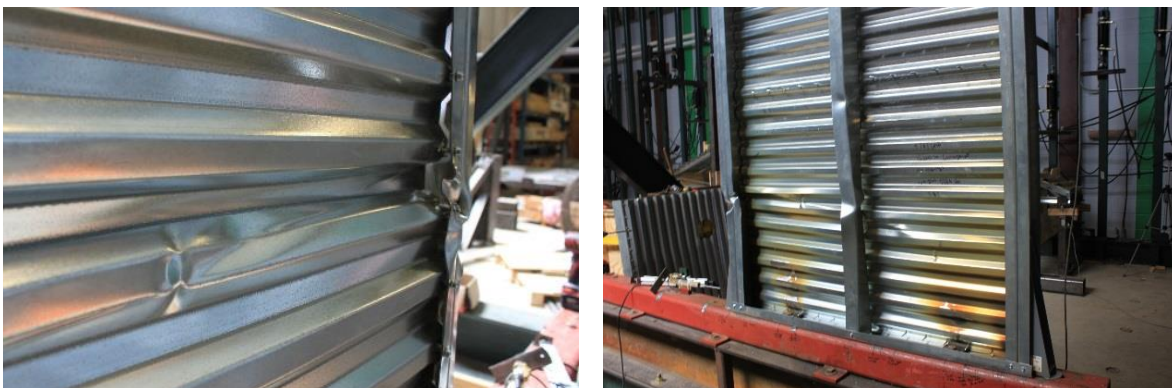


(a) Tension Side

(b) Compression Side

Fig. 4: Failures of Bearing Wall Specimen under Monotonic Loading

For the shear wall under monotonic loading, the vertical chord tracks did not lift up on the tension side due to the hold-downs being in place. Local buckling in the vertical chord tracks on the compression side was observed right above the hold-down, as shown in Fig. 5. This failure was not observed in Mahdavian's (2016) research, where no gravity loads were applied on the shear walls. The reason of the new failure mode was believed to be the second-order effects. Other failures observed were screws pull-out on the bottom corrugated steel sheet, field vertical track local buckling. The loading was terminated at 7.5% drift and the shear walls were capable of carrying the gravity load without collapse during the whole loading process. The failures of the shear wall specimen in monotonic test are shown in Fig. 5.



(a) Screw pull-out

(b) Local Buckling of Framing Members

Fig. 5: Failures of the Shear Wall Specimen in Monotonic Test

2.5.2 Wall Behaviors under Cyclic Loading

For bearing wall specimens under cyclic loading, vertical chord tracks buckled at the bottom ends at cycle 38 during the test. Unlike bearing wall in the monotonic test, screw pull-out was observed between the vertical chord track and the bottom track connection. Maximum drift in the cyclic test reached 4.79% and the bearing walls were able to carry gravity load without collapse during the test. The failures of the bearing wall specimen in cyclic test are shown in Fig. 6.



Fig. 6: Failure Modes of the Bearing Wall Specimen in Cyclic Test

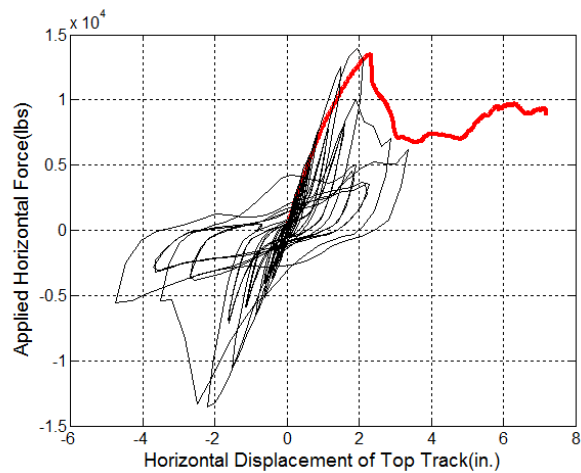
For the first shear wall specimen in the cyclic tests, both vertical chord tracks buckled above hold-down. For the second shear walls specimen, minor local buckling was observed on the vertical chord tracks. For both tests, screws broke and screw pull-out were observed on the middle and bottom sheets. Screw pull-out at the sheathing overlap between middle sheet and bottom sheet was also observed. The failures of the shear wall specimen under cyclic loading are shown in Fig. 7.



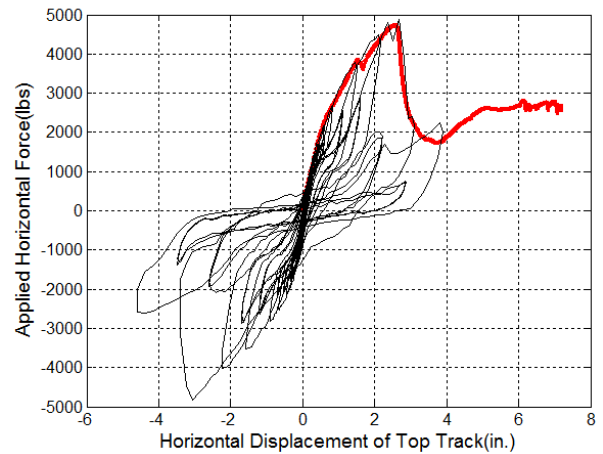
Fig. 7: Failures of the Shear Wall Specimen in Cyclic Test

2.5.3 Test Results and Discussion

The results of each specimen under monotonic and cyclic loadings are summarized in Table 3. Ductility factor was calculated using the equivalent energy elastic plastic model (EEEP) according to AISI S213 (2012). Typical bearing wall test and shear wall test curves under monotonic and cyclic loading are shown in Fig. 8.



(a) Shear wall Test results



(b) Bearing wall Test results

Fig. 8: Test Result Curves

It is important to discuss the lateral resistance contribution of the bearing wall to the lateral force resistance system. The bearing walls under monotonic loading and cyclic loading were able to resist the equivalent of approximately 36% of the shear resistance of the shear wall. Considering the number of bearing walls in CFS structures, their contribution to the lateral-force-resisting system should not be ignored.

Table 3: Test Results of Sheet-in Bearing Wall and Sheet-in Shear Wall

Test label	Wall type	Test protocol (M/C)	Hold-down	Average Peak Load (plf)	Average Disp. @ Peak Load (in.)	Ductility Factor	Drift	Initial Stiffness k (lbs/in.)
4x8x68x27 - T#1	Bearing Wall	M	N	1187	2.58	2.87	7.50%	4066
4x8x68x27 - T#1	Shear wall	M	Y	3381	2.30	1.80	7.50%	8561
4x8x68x27 - T#1	Bearing wall	C	N	1380	3.02	2.09	3.15%	2845
4x8x68x27 - T#2	Bearing wall	C	N	1212	2.87	3.99	2.98%	4561
4x8x68x27 - T#1	Shear wall	C	Y	3459	2.12	2.01	2.21%	8493
4x8x68x27 - T#2	Shear wall	C	Y	3587	2.10	2.20	2.19%	10461

Note: plf – pound per linear foot

In addition, the 7% collapse drift limit of the sheet-in wall system was considered appropriately. The bearing walls and shear walls were able to carry the gravity loads without collapse through the loading process at a maximum drift of 7.5%. In Chapter 9 of FEMA P695 (2009), the Example adopts a 7% drift as the collapse drift limit for the light wood framed structures. FEAM P695 does not provide a recommended drift limit for light steel framed structures. However, these two CFS framed structure systems were considered to have similar seismic behaviors by the research communities. For instance, the same seismic performance factors were adopted on both structure systems in IBC (2015) and ASCE -7 (2010). Also, Zhang (2016) considered a

collapse drift limit of 7% as appropriate and conservative for the CFS structure system with sheet-out shear walls. As a result, this study adopted a 7% drift limit as the collapse drift limit in the following numerical analysis and seismic performance evaluation.

3. Finite Element Modeling

3.1 Building Archetype

FEMA P695 (2009) describes that a building archetype is a prototypical representation of a seismic-force-resisting system. Archetypes are intended to reflect the wide range of design parameters and building attributes. The archetype can be assembled into performance groups based on their major differences in plan configuration, building height, building occupancy, design gravity, seismic load intensity, etc. This study referenced Zhang's office archetype model for seismic performance analysis, as shown in Fig. 9 and Table 4. A total of 3 office building archetypes vary in building height (number of stories) were selected in this study. The detailed building model information can be found at Appendix B of Lan's (2017) thesis. The following assumptions are briefly made in the archetype definition:

(1) Building occupancy: The office building archetype dimensions are 49.9 ft \times 23 ft (15.2m \times 7m) which is similar to an archetype designed in the NEES-CFS project (Madsen, Nakata, Schafer, 2011). All shear walls and bearing walls are placed along the exterior side in the office building archetype. Fig. 9 illustrates the plan layouts of the office building archetypes.

(2) Number of stories: Building stories vary from 2-story to 5-story. Per Table 504.4 in IBC (2015), building constructed with noncombustible material can increase the building height from 3 stories to 5 stories. As a result, 5-story is considered as the maximum story on building archetypes.

(3) Seismic design category (SDC): the archetypes are assumed to be designed in SDC D per ASCE 7-16 (2016). The Maximum Considered Earthquake (MCE) spectral response acceleration parameter for short-period $S_{ms}=1.39g$ was used for the office structure.

(4) Design Criteria: Load Resistance Factor Design (LRFD) was applied in the design of lateral force resisting system and the seismic force modification factors were based on the light-frame steel shear resistance systems with flat steel sheathing (ASCE 7-16). $R = 6.5$ and $\Omega = 3.0$ were initially used in the building archetype design and were subject to be evaluated in this study.

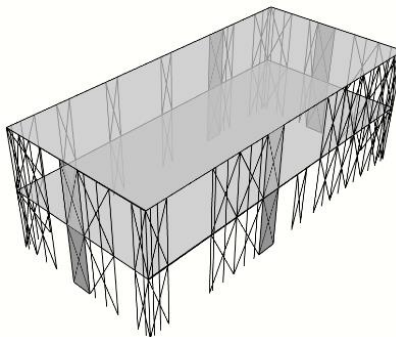


Fig. 9: Building Archetype Plan Layouts

Table 4: Three Office Building Archetypes

Arch. ID	No. of Stories	Key Archetype Design Parameters				
		Occupancy	Shear wall Aspect Ratio	S_{MT}^1 (g)	T^2 (s)	$(V/W)^3$ (g)
1	2	Office	2.57	1.39	0.245	0.143
2	3	Office	2.57	1.39	0.332	0.143
3	5	Office	2.57	1.39	0.486	0.143

Notes: 1. S_{MT} - Maximum considered earthquake spectral acceleration.
 2. T - Fundamental period calculated according to Section 5.2.5 in FEMA P695 (2009).
 3. $V/W = C_s$, seismic response coefficient.

3.2 Design of Shear Walls

Earthquake loads were calculated in accordance with Chapter 11 of ASCE 7-10, and vertical distribution of seismic forces and number of shear walls were determined afterwards. A detailed example of shear walls design can be found in Lan's (2017) thesis.

The nominal shear wall strength was based on the average test results reported herein. It should be noted that the width of the shear wall used in the building archetype was 3.5 ft. wide, which was different from test specimens with 4 ft. width. Per AISI S240 (2015), for Type I shear walls with aspect ratios (h/w) greater than 2:1 but no exceeding 4:1, the nominal strength shall be multiplied by $(2w/h)$. In addition, a resistance factor of $\phi = 0.6$ was considered according to the provisions in AISI S400 (2015).

3.3 Modeling of Shear Walls

3.3.1 Modeling of Shear Walls

The shear wall was simulated in OpenSees as two diagonal truss elements and elastic beam-column elements as illustrated in Fig. 10. EqualDOF command was used to ensure the displacement of the top two ends of the wall were the same.

Pinching effect is a load-deformation response and exhibits stiffness and strength degradation under cyclic loading. To achieve the pinching effect, pinching4 uniaxial hysteretic material was used for the diagonal truss elements. To obtain the backbone curve of pinching4 material, the relationship of load and displacement in the horizontal direction was first converted to the stress and strain in the truss elements.

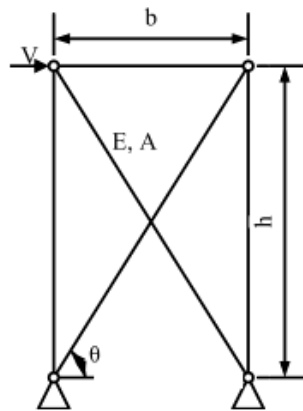


Fig. 10: Shear wall Numerical Model

The axial force in the diagonal truss element F can be expressed as:

$$F = \frac{V}{2(\cos \theta)} \quad (1)$$

The stress and strain in the diagonal truss element are calculated as:

$$\sigma = \frac{F}{A} = \frac{V}{2A(\cos \theta)} \quad (2)$$

$$\varepsilon = \frac{d}{l} = \frac{\Delta \cos \theta}{l} \quad (3)$$

Where $\cos \theta = \frac{b}{\sqrt{b^2+h^2}}$, and $l = \sqrt{b^2 + h^2}$. Variables b and h are the width and height of the shear wall respectively.

After the backbone curve is defined by 4 positive and 4 negative points, it is required to input the parameters that can define the strength, stiffness degradation and pinching effect under cyclic loading, as shown in Fig. 11. The complete set of Pinching4 parameters can be found in Lan's (2017) thesis. The definition of the parameters can be found in the OpenSees Command Manual.

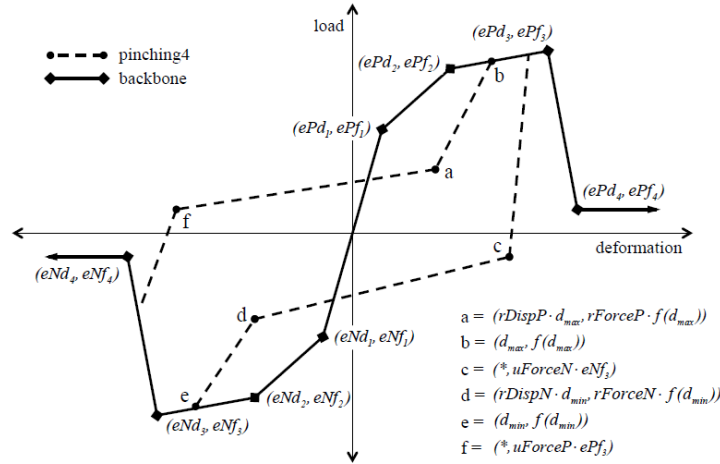


Fig. 11: The Parameter Definition of Pinching4 Material

The comparison between the shear wall simulation results and the shear wall test results are shown in Fig. 12. It can be concluded that the simulation results and test results are in good agreement. Also, the shear wall model is able to simulate the post-peak behaviors of the shear wall test. Note that only the last 15 cycles of the 43 test cycles are plotted in Fig. 12 as they are the most important cycles as the shear wall still performed under elastic stage in the previous cycles.

3.4 Modeling of Diaphragm

Leng's dissertation (2015) concluded that the stiffness of diaphragms contributes greatly to the overall stiffness of 3D models and determines the extent of coupling between shear walls. Per the

modeling guidelines in Leng’s (2015) research, modeling diaphragms as rigid was simpler and was a better initial assumption. This study referred Leng’s guideline and modeled floor and roof diaphragm as ridged diaphragm, so did Zhang (2016).

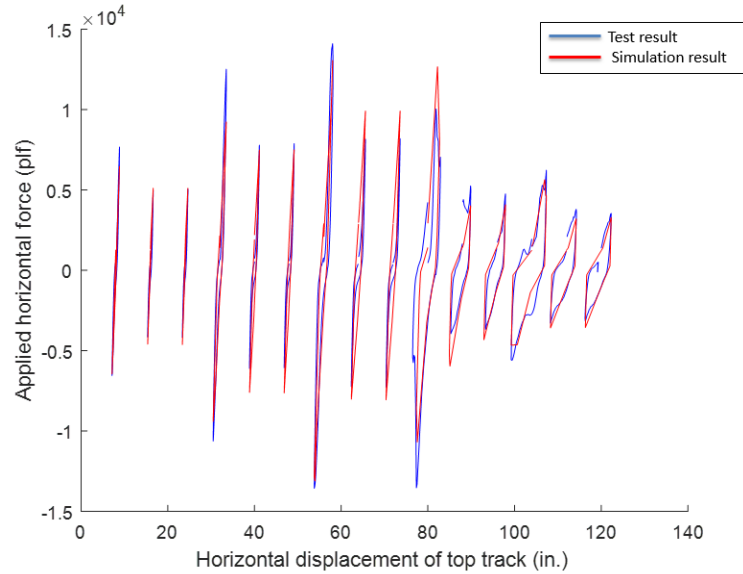


Fig. 12: Comparison between Shear Wall Simulation Results and Test Results

3.5 Seismic Mass and Gravity Load

For office building, total seismic mass was referred to the effective seismic mass calculated in the Design Narrative (Madsen, Nakata, Schafer, 2011). The mass on each floor was divided equally and lumped to the four corners of the building model. Since gravity loads has been applied in the test, which means P-delta effects has been reflected in the test results. So, no P-delta effect was defined in the model.

3.6 Nonlinear Static (Pushover) Analysis

The objective of nonlinear static (pushover) analysis was to quantify maximum base shear strength, V_{max} , effective yield roof drift displacement, $\delta_{y,eff}$ and ultimate roof displacement, δ_u . The applied lateral force at each story level was in proportion to the fundamental mode shape of the index archetype model. The overstrength factor for a given index archetype model is defined as $\Omega_0 = V_{max}/V_{design}$, where, V_{max} , is the maximum base shear in actual behavior and V_{design} is base shear at design level. The displacement ductility factor is defined as $\mu_T = \delta_u/\delta_{y,eff}$, where displacement, δ_u , is taken as the roof displacement at the point of 20% strength loss ($0.8 V_{max}$), and the effective yield roof drift displacement $\delta_{y,eff}$ is per Equation 6-7 in FEMA-P695. The typical pushover curves of the 2-story office building in both directions are shown in Fig. 13. The detailed pushover results are summarized in Table 5. Pushover analysis on other building archetypes can be found in Appendix D in Lan’s (2017) thesis.

Table 5: Pushover Results of 2-Story Office Building Models

Direction	T (s)	$T1$ (s)	δ_u (in.)	$\delta_{y,eff}$ (in.)	V_{max} (kips)	V_{design} (kips)	μ_t	Ω_0
Long	0.244	0.470	4.2	2.34	66.79	11.06	1.82	6.04
Short	0.244	0.580	4.37	2.50	46.86	11.06	1.75	4.24

scaled to increasing spectral intensity. It can be seen that S_{CT} is 2.42 (g), and S_{MT} is 1.39 (g) in Fig. 14-a.

Another expression of IDA result is the fragility curve. Fragility curve can be defined through a cumulative distribution function, which relates the ground motion intensity to the probability of collapse. (Ibarra et al., 2002). Fig. 14-b shows fragility curve of the 2-story office building in the long direction by fitting a lognormal distribution through the collapse data points from Fig. 14-a. In Fig. 14-b, the S_{CT} corresponds the 50% collapse probability of the index archetype at the ground motion intensity S_{CT} . Therefore, CMR can be calculated as $S_{CT}/S_{MT} = 2.42/1.39 = 1.74$. IDA analysis on other building archetypes can be found in Appendix D in Lan's (2017) thesis.

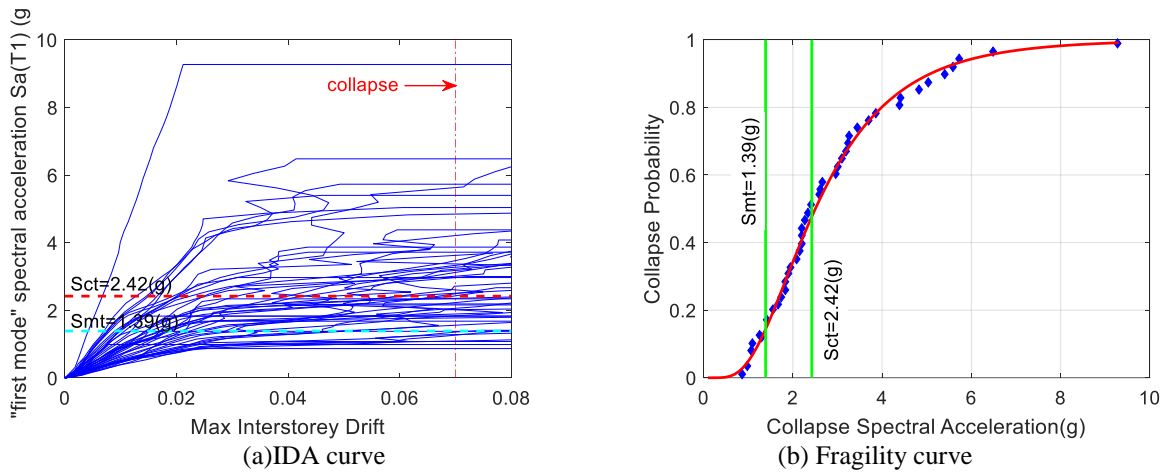


Fig. 14: IDA Results of the 2-Story Office Building in the Long Direction

4. Seismic Performance Evaluation

This section discusses the process of evaluating the seismic performance of newly proposed sheet-in shear wall seismic-force-resisting system, assessing the acceptable trial value of the response modification coefficient, R , determining appropriate values of the system overstrength factor Ω_0 , and the deflection amplification factor, C_d .

In general, trial values of seismic performance factors are evaluated for each building archetype. The results within each performance group are averaged to determine the value for the group, which is the primary basis for judging acceptability of the trial value. The detailed process of performance evaluation process can be found in Section 7.1 of FEMA P695.

The CMR value has to be adjusted to Adjusted Collapse Margin Ratio, ACMR, for each index archetype due to influence of the unique spectral shape (frequency content) of rare ground motions. In addition, many sources of uncertainty contribute to variability in collapse capacity, it is important to incorporate their effects in the collapse assessment process. Four kinds of uncertainty, all together called total system uncertainty, β_{TOT} , were considered in the performance evaluation process, there were record-to-record uncertainty (RTR), design requirements uncertainty (DR), test data uncertainty (TD), and modeling uncertainty (MDL). Based on the uncertainty assessment criteria, this study rated the design requirements uncertainty, test data uncertainty and modeling uncertainty were good, while record-to-record

uncertainty was a function of displacement ductility factor μ_T , its calculation can be found in Equation 7-2 of FEMA P695. The detailed argument for these 4 uncertainties ratings can be found in Lan's (2017) thesis.

Acceptable values of adjusted collapse margin ratio are based on total system collapse uncertainty, β_{TOT} , and established values of acceptable probabilities of collapse, which can be found in Table 6-3 of FEMA P695.

The acceptable response modification coefficient requires each index archetype and each performance group meet the following two criteria: individual values of adjusted collapse margin ratio for each index archetype within a performance group exceeds $ACMR_{20\%}$, i.e., $ACMR_i \geq ACMR_{20\%}$; and the average value of adjusted collapse margin ratio for each performance group exceeds $ACMR_{10\%}$, i.e., $\overline{ACMR}_i \geq ACMR_{10\%}$.

The average value of archetype overstrength, Ω , is calculated for each performance group. Then, the value of the system overstrength factor, Ω_0 , for use in design should not be taken as less than the largest average value of calculated archetype overstrength, Ω , from any performance group.

The deflection amplification factor, C_d , is based on the acceptable value of the response modification factor, R , reduced by the damping factor, B_I . Its equation is $C_d = \frac{R}{B_I}$, where B_I is the numerical damping coefficient given in Table 18.6-1 of ASCE 7-10 (2016). However, the inherent damping of the newly proposed CFS framed building system with sheet-in shear wall needs to be verified by future investigations. According to the test results by Shafer (2015), the measured damping of the CFS framed building using wood sheathed shear walls varied from 4% to 9%. This study adopted 5% inherent damping in this research, which was believed to be appropriate. As a result, the damping coefficient, B_I , equals to 1.0, which makes C_d equal to R .

4.1 Seismic Performance Evaluation Results of Office Archetypes

The results of the performance evaluation of the office performance group are summarized in Table 6. Detailed calculations of the archetypes performance evaluation can be found at Appendix B & D in Lan's (2017) thesis.

4.2 Summary of Performance Evaluation

For performance evaluation based on the good uncertainty ratings, all individual values of adjusted collapse margin ratio (ACMR) for each index archetype within a performance group exceeded the corresponding $ACMR_{20\%}$ value. And the average value of adjusted collapse margin ratio (ACMR) for each performance group exceeded the corresponding $ACMR_{10\%}$ value. This proved that the trial value of the response modification coefficient, $R=6.5$, was acceptable.

The average value of overstrength factor, Ω_0 , are 3.73 for office building group. According to the Section 7.6 in FEMA P695, a practical limit on the value of Ω_0 is about 3.0, which is consistent with the largest value of this factor specific in Table 12.2-1 of ASCE 7-10 for all currently approved seismic-force-resisting systems. Hence, this study proposed the use of 3.0 for overstrength factor as the average value of each performance group. Lastly, the deflection amplification factor, C_d , was equal to the value of R due to the value of B_I equals to 1.0, which has been discuss in the previous section.

Table 6: Performance Evaluation Results of the Office Building Archetypes

	Ω_0	μ_t	S_{CT}	S_{MT}	CMR	SSF	ACMR	β_{TOR}	Accept ACMR(20%)	Accept ACMR(10%)	
Office building	2-story-long	6.04	1.82	2.42	1.39	1.741	1.119	1.948	0.447	1.458	1.775
	2-story-short	4.24	1.75	2.42	1.39	1.741	1.116	1.943	0.444	1.441	1.742
	3-story-long	4.1	1.83	2.83	1.39	2.036	1.12	2.279	0.448	1.458	1.775
	3-story-short	3.22	1.62	2.53	1.39	1.82	1.107	2.015	0.434	1.441	1.742
	5-story-long	2.67	2.52	2.53	1.39	1.82	1.156	2.104	0.494	1.513	1.886
	5-story-short	2.1	2.19	2.31	1.39	1.662	1.141	1.896	0.471	1.485	1.83
Mean of Office Performance Group	3.73	1.96	2.51	1.39	1.803	1.127	2.031	0.456	1.466	1.792	

5. Conclusion

This study was a follow-up to Mahdavian's (2016) and Zhang's (2016) research, the objective was to further study the structural performance of the newly designed sheet-in shear wall lateral-force-resisting system, and its potential application in mid-rise buildings.

Compared to sheet-out shear wall, sheet-in shear wall provides a smooth surface so that it is easier for the installation of panels and finishes. In this study, it was the first time to test the sheet-in shear walls under combined lateral and gravity loads. The monotonic and cyclic test results showed local buckling of the chord framing members above the hold-downs. The test results also showed that the strength of the sheet-in bearing wall was approximately one third of the strength of the sheet-in shear wall. If a structure has large number of bearing walls, their contribution to the lateral force resisting system could be significant. In the monotonic tests, it was observed that both sheet-in shear walls and bearing walls were able to carry gravity load without collapse at the maximum drift of 7.5% so that 7% drift was conservatively set as the collapse drift limit for the sheet-in shear wall in the numerical model.

The seismic performance evaluation was performed on office building archetypes by following the methodology in FEMA P695. Nonlinear static and dynamic analysis were performed in both horizontal directions of each building archetype. The results of the performance evaluation verified the seismic performance factors ($R=C_d=6.5$ and $\Omega=3.0$) were appropriate for the sheet-in shear wall system based on good uncertainty ratings, which is consistent with the seismic performance factor used in CFS framed shear wall with flat steel sheet and wood-based panel. Implementation of the methodology in FEMA P695 involves uncertainty, judgment and other variations. All the documentations and the proposed seismic performance factors shall be reviewed by an independent peer review panel before the adoption of the proposed seismic performance factors for this newly design sheet-in shear wall system.

Acknowledgements

This paper was prepared as part of the U.S. National Science Foundation grant, NSF-CMMI-0955189: Comprehensive Research on Cold-Formed Steel Sheathed Shear Walls, Special Detailing, Design, and Innovation. Any opinions, findings, and conclusions or recommendations expressed in this article are those of the authors and do not necessarily reflect the views of the sponsors.

The presented wall design is currently in a pending US patent application 15/466,983.

References

- AISI S100(2012). “North American specification for the design of cold formed steel structural members.” Washington, D.C.: *American Iron and Steel Institute*.
- AISI S240(2015). “North American Standard for Cold-Formed Steel Structural Framing.” Washington, D.C.: *American Iron and Steel Institute*.
- AISI S400(2015). “North American Standard for Seismic Design of Cold-Formed Steel Structural Systems”. Washington, D.C.: *American Iron and Steel Institute*.
- ASCE 7 (2010). “Minimum design loads for buildings and other structures.” Reston, VA: *American Society of Civil Engineers*.
- ASTM A325 (2007). “A325-07 Standard Specification for Structural Bolts, Steel, Heat Treated, 120/105 ksi Minimum Tensile Strength.” West Conshohocken, PA.: *American Society for Testing and Materials*.
- ASTM A370(2006). “A370-06 Standard Test Methods and Definitions for Mechanical Testing of Steel Products.” West Conshohocken, PA.: *American Society for Testing and Materials*.
- ASTM A490(2008). “A490-08 Standard Specification for Structural Bolts, Steel, Heat Treated, 150 ksi Minimum Tensile Strength”. West Conshohocken, PA: *American Society for Testing and Materials*.
- ASTM E564(2012). “Standard Practice for Static Load Test for Shear Resistance of Framed Walls for Buildings.” West Conshohocken, PA.: *American Society for Testing and Materials*.
- Data, A. P. (2012). “AISI Standard for Cold-Formed Steel Framing _ Product Data 2012 Edition.” Washington, D.C.: *American Iron and Steel Institute*.
- Dubina, F. a. (2004). “Performance of wall-stud cold-formed shear panels under monotonic and cyclic loading Part I: Experimental research”. *Thin-Walled Structures*, 42 (2004) 321-338.
- FEMA P695 (2009). “Qualifications of Building Seismic Performance Factors.” Washington, D.C.: *Federal Emergency Management Agency*.
- Foliente GC, “Issues in seismic performance testing and evaluation of timber structural systems[C].” *International Wood Engineering Conference*, New Orleans LA, 1996, 1:29-36.
- IBC (2015). “International Building Code, 2015 Edition.” Washington, D.C.: *International Code Council*.
- Leng, J. (2015). “Simulation of Cold-formed Steel Structures.” Baltimore, MD: PhD Dissertation, *Johns Hopkins University*.
- Madsen, R. N. (2011). “CFS-NEES Building Structural Design Narrative.” www.ce.jhu.edu/cfsness.
- Mahdavian, M. (2016). “Innovative Cold-Formed Steel Shear Walls With Corrugated Steel Sheathing.” Denton, TX: Thesis, *University of North Texas*.
- McKenna, F. e. (2015). “Open system for earthquake engineering simulation (OpenSees).” Berkeley, CA: *Pacific Earthquake Engineering Research Center*.
- Park, “Evaluation of ductility of structures and structural assemblages from laboratory testing.” *Bulletin of the New Zealand national Society of Earthquake Engineering*, 1989, 22(3): 155-166.
- Peterman, K. D. (2014). “Experimental seismic behavior of the CFS-NEES building: system-level performance of a full-scale two-story light steel framed building.” *Proceedings of 22nd International Specialty Conference on Cold-Formed Steel Structures*, (pp. 887-901). St. Louis, MO.
- Stojadinovic and Tipping(2007). “Structural testing of corrugated sheet steel shear walls.” Ontario, CA: *Report submitted to Charles Pankow Foundation*.
- Yu, C., Huang, Z., Vora, H.(2009). “Cold-Formed Steel Framed Shear Wall Assemblies with Corrugated Sheet Steel Sheathing.” *Proceedings of the Annual Stability Conference*. Phoenix, AZ: Structural Stability Research Council.
- Yu, G. (2013). “Cold-Formed Steel Framed Shear Wall Sheathed with Corrugated Steel Sheet.” Denton, TX: Thesis, *University of North Texas*.
- Zhang, W. Mahdavian, M., Li, Y., and Yu, C. (2016). “Experiments and Simulations of Cold-Formed Steel Wall Assemblies Using Corrugated Steel Sheathing Subjected to Shear and Gravity Loads.” *Journal of Structural Engineering*, Vol. 143, Issue 3.
- Zhang, W. Mahdavian, M., Li, Y., and Yu, C. (2017). “Seismic Performance Evaluation of Cold-Formed Steel Shear Walls Using Corrugated Sheet Sheathing.” *Journal of Structural Engineering*.